ISO TC 20/SC 14

Date: 2010-09-7

ISO 27852:2010(E)

ISO TC 20/SC 14/WG 3

Secretariat: ANSI

Space systems — Estimation of orbit lifetime

Élément introductif — Élément central — Élément complémentaire

Document type: International Standard
Document subtype:
Document stage: (60) Publication
Document language: E

J:\1Earth_Proprietary\1Earth_Proprietary_Library\Professional_Societies\ISO_TC20_SC14\Orbit_Lifetime\27852_Std_Final_Version\ISO_27852_(E)4.doc STD Version 2.1c2

Contents

Page

Foreword

ISO (the International Organization for Standardization) is a worldwide federation of national standards bodies (ISO member bodies). The work of preparing International Standards is normally carried out through ISO technical committees. Each member body interested in a subject for which a technical committee has been established has the right to be represented on that committee. International organizations, governmental and non-governmental, in liaison with ISO, also take part in the work. ISO collaborates closely with the International Electrotechnical Commission (IEC) on all matters of electrotechnical standardization.

International Standards are drafted in accordance with the rules given in the ISO/IEC Directives, Part 2.

The main task of technical committees is to prepare International Standards. Draft International Standards adopted by the technical committees are circulated to the member bodies for voting. Publication as an International Standard requires approval by at least 75 % of the member bodies casting a vote.

ISO 27852 was prepared by Technical Committee ISO/TC 20, *Aircraft and space vehicles*, Subcommittee SC 14, *Space systems and operations*.

Introduction

A spacecraft is exposed to the risk of collision with orbital debris and operational satellites throughout its launch, early orbit and mission phases. This risk is especially high during passage through or operations within the LEO region.

To address these concerns, the Inter-Agency Space Debris Coordination Committee (IADC) recommended to the United Nations[1] (section 5.3.2 'Objects Passing Through the LEO Region'): "Whenever possible space systems that are terminating their operational phases in orbits that pass through the LEO region, or have the potential to interfere with the LEO region, should be de-orbited (direct re-entry is preferred) or where appropriate manoeuvred into an orbit with a reduced lifetime. Retrieval is also a disposal option." and "A space system should be left in an orbit in which, using an accepted nominal projection for solar activity, atmospheric drag will limit the orbital lifetime after completion of operations. A study on the effect of post-mission orbital lifetime limitation on collision rate and debris population growth has been performed by the IADC. This IADC and some other studies and a number of existing national guidelines have found 25 years to be a reasonable and appropriate lifetime limit."

The Scientific and Technical Subcommittee (STSC) of the United Nations Committee on the Peaceful Uses of Outer Space (UNCOPUOS), acknowledging the benefits of the IADC guidelines, established the Working Group on Space Debris to develop a set of recommended guidelines[2] based on the technical content and the basic definitions of the IADC space debris mitigation guidelines, taking into consideration the United Nations treaties and principles on outer space. Consistent with the IADC recommendations (listed above), STSC Guideline 6 states that space mission planners, designers, manufacturers and operators should "Limit the long-term presence of spacecraft and launch vehicle orbital stages in the low-Earth orbit (LEO) region after the end of their mission." STSC guidelines also state, "For more in-depth descriptions and recommendations pertaining to space debris mitigation measures, Member States and international organizations may refer to the latest version of the IADC space debris mitigation guidelines and other supporting documents, which can be found on the IADC website (www.iadc-online.org)."

The purpose of this standard is to provide a common, consensus approach to determining orbit lifetime, one that is sufficiently precise and easily implemented for the purpose of demonstrating compliance with IADC guidelines. This project offers standardized guidance and analysis methods to estimate orbital lifetime for all LEO-crossing orbit classes.

This standard is a supporting document to ISO 24113[3], Space systems -- Space debris mitigation requirements, and the GEO and LEO disposal standards that are derived from ISO 24113.

Space systems — Estimation of orbit lifetime

1 Scope

This standard describes a process for the estimation of orbit lifetime for satellites, launch vehicles, upper stages and associated debris in LEO-crossing orbits.

The international standard also clarifies the following:

i) modelling approaches and resources for solar and geomagnetic activity modelling;

ii) resources for atmosphere model selection;

iii) approaches for satellite ballistic coefficient estimation.

2 Terms, definitions, symbols and abbreviated terms

2.1 Terms and definitions

For the purposes of this document, the following terms and definitions apply.

2.1.1
orbit lifetime
elapsed time between the orbiting satellite's initial or reference position and orbit demise/reentry

NOTE 1 An example of the orbiting satellite's reference position is the post-mission orbit.

NOTE 2 The orbit's decay is typically represented by the reduction in perigee and apogee altitudes (or radii) as shown in Figure 1.

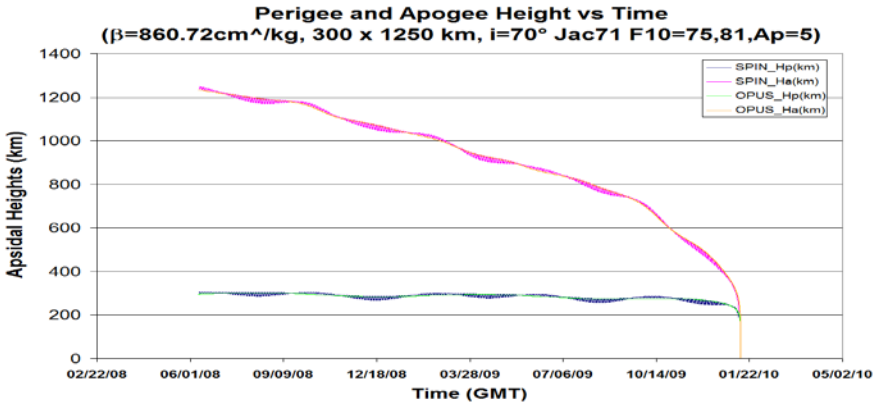

Figure 1 — Sample of orbit lifetime decay profile

2.1.2
disposal phase
interval during which a spacecraft or launch vehicle orbital stage completes its disposal actions.

2.1.3
earth equatorial radius
equatorial radius of the Earth

NOTE The equatorial radius of the Earth is taken as 6,378.137 km and this radius is used as the reference for the Earth's surface from which the orbit regions are defined.

2.1.4
LEO-crossing orbit
Low-Earth Orbit, defined as an orbit with perigee altitude of 2000 km or less

NOTE As can be seen in Figure A.1, orbits having this definition encompass the majority of the high spatial density spike of satellites and space debris.

2.1.5
long-duration orbit lifetime prediction
orbit lifetime prediction spanning two solar cycles or more (e.g., 25-year orbit lifetime)

2.1.6
mission phase
phase where the space system fulfills its mission

NOTE Begins at the end of the launch phase and ends at the beginning of the disposal phase.

2.1.7
post-mission orbit lifetime
duration of the orbit after completion of the mission phase

NOTE The Disposal Phase duration is a component of Post-Mission duration.

2.1.8
satellite
system designed to perform specific tasks or functions in outer space

NOTE A spacecraft that can no longer fulfill its intended mission is considered non-functional. Spacecraft in reserve or standby modes awaiting possible reactivation are considered functional).

2.1.9
space debris
all man-made objects, including fragments and elements thereof, in Earth orbit or re-entering the atmosphere, that are non-functional.

2.1.10
space object
man-made object in outer space.

2.1.11
orbit
path followed by a space object.

2.1.12
solar cycle
≈11-year solar cycle based on the 13-month running mean for monthly sunspot number and is highly correlated with the 13-month running mean for monthly solar radio flux measurements at the 10.7cm wavelength

NOTE 1 Historical records back to the earliest recorded data (1945) are shown in Figure 2.

NOTE 2 For reference, the current 25-year post-mission IADC orbit lifetime recommendation is overlaid onto the historical data; it can be seen that multiple solar cycles are encapsulated by this long time duration.

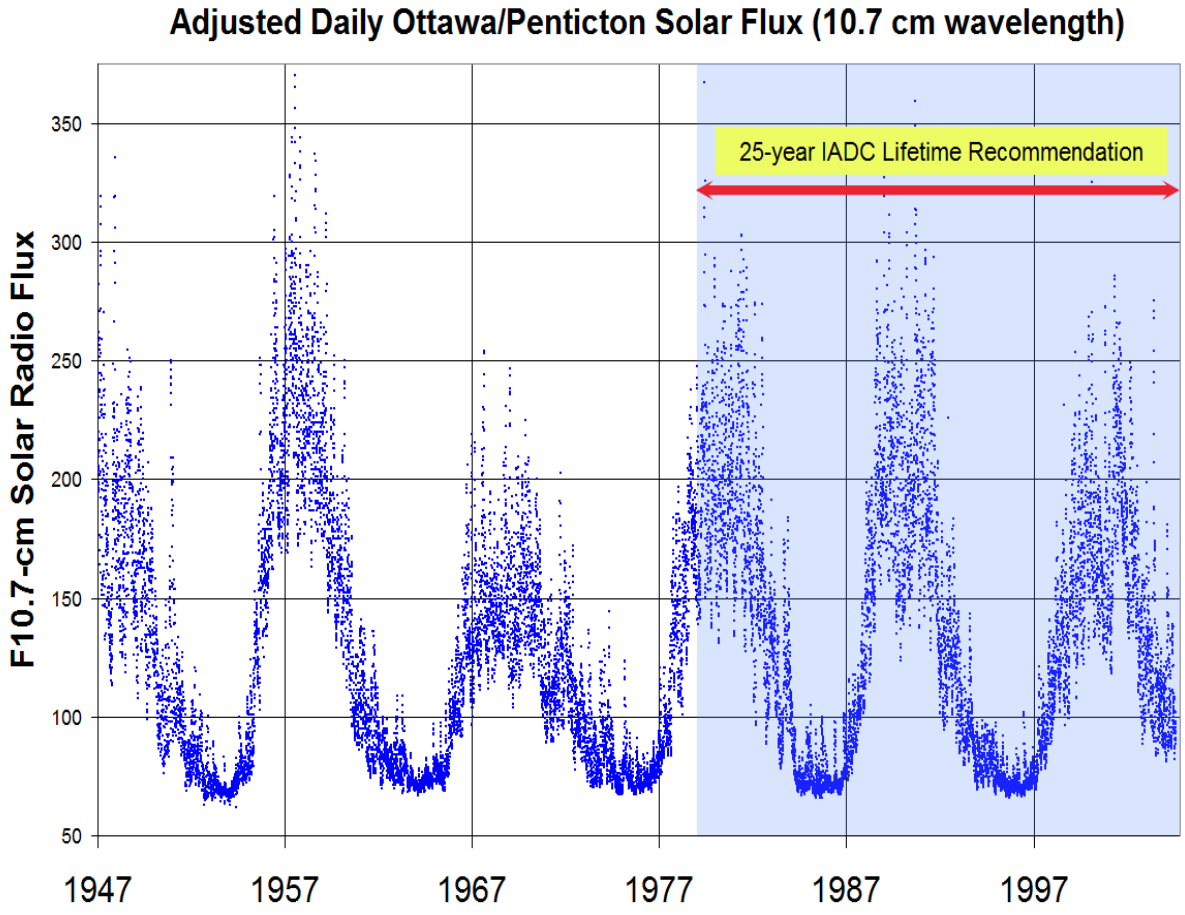

Figure 2 — Solar cycle (≈11-year duration)

2.2 Symbols

a	Orbit semi-major axis
A	Satellite cross-sectional area with respect to the relative wind
A_p	Earth daily geomagnetic index
β	Ballistic coefficient of satellite = $C_D * A / m$
C_D	Satellite drag coefficient
C_R	Satellite reflectivity coefficient

e	Orbit eccentricity
$F_{10.7}$	Solar radio flux observed daily at 2800 MHz (10.7 cm) in solar flux units (10^{-22}W m^{-2} Hz^{-1})
$F_{10.7}$ *Bar*	Solar radio flux at 2800 MHz (10.7 cm), averaged over three solar rotations
H_a	Apogee altitude = a (1 + e) - R_e
H_p	Perigee altitude = a (1 – e) - R_e
m	Mass of satellite
R_e	Equatorial radius of the Earth

2.3 Abbreviated terms

GEO	Geosynchronous Earth Orbit
GTO	Geosynchronous Transfer Orbit
IADC	Inter-Agency Space Debris Coordination Committee
ISO	International Organization for Standardization
LEO	Low Earth Orbit
RAAN	Orbit Right Ascension of the Ascending Node (the angle between the vernal equinox and the orbit ascending node, measured CCW in the equatorial plane, looking in the –Z direction).
STSC	Scientific and Technical Subcommittee of the Committee
UNCOPUOS	United Nations Committee on the Peaceful Uses of Outer Space

3 Orbit lifetime estimation

3.1 General requirements

The orbital lifetime of LEO-crossing mission-related objects shall be estimated using the processes specified in this document. In addition to any user-imposed constraints, the post-mission portion of the resulting orbit lifetime estimate shall then be constrained to a maximum of 25 years per IADC recommendations using a combination of (1) initial orbit selection; (2) satellite vehicle design; (3) spacecraft launch and early orbit concepts of operation which minimize LEO-crossing objects; (4) satellite ballistic parameter modifications at EOL; and (5) satellite deorbit maneuvers.

3.2 Definition of orbit lifetime estimation process

The orbit lifetime estimation process is represented generically in Figure 3.

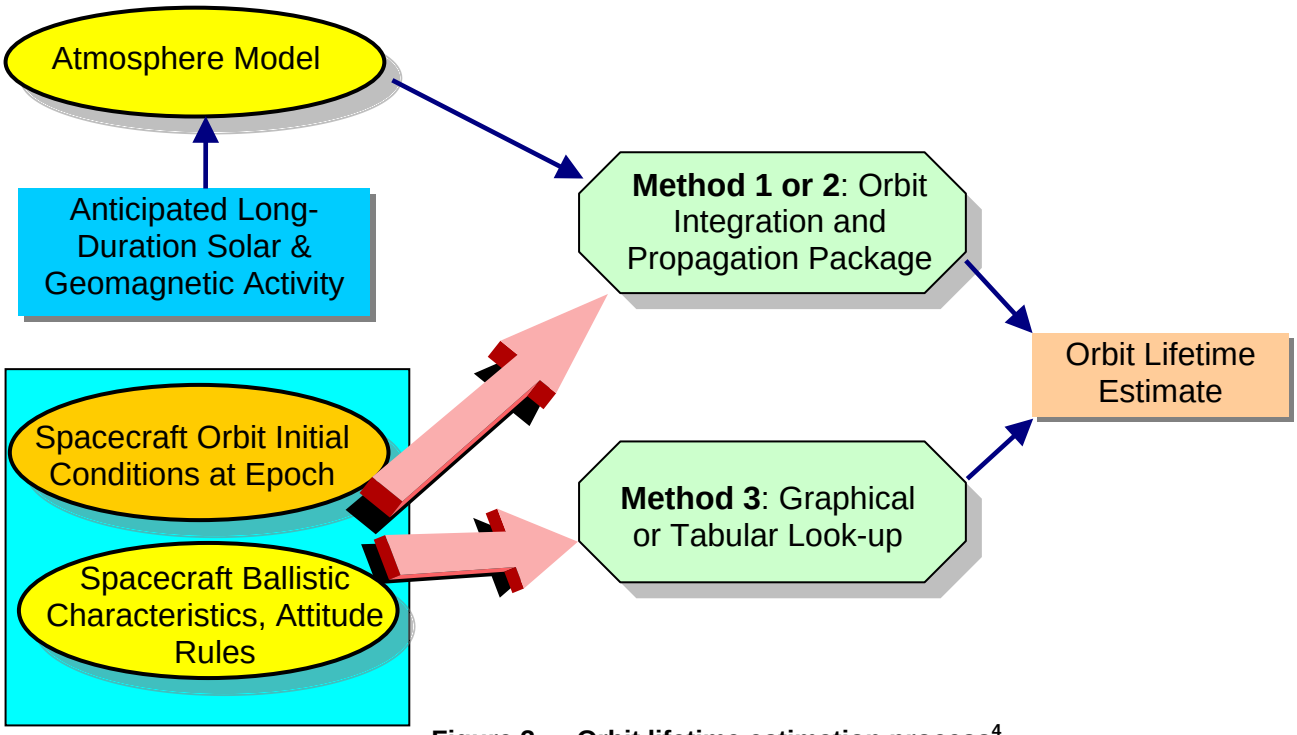

Figure 3 — Orbit lifetime estimation process[4]

4 Orbit lifetime estimation methods and applicability

4.1 General

There are three basic analysis methods used to estimate orbit lifetime[4], as depicted in Figure 3. Determination of the method used to estimate orbital lifetime for a specific space object shall be based upon the orbit type and perturbations experienced by the satellite as shown in Figure 4.

	Special Orbit:		Conservative Margin Applied to Each Method:			
Orbit Apogee Altitude (km)	**Sun-Sync?**	**High Area-to-mass?**	**Method 1: Numerical Integration**	**Method 2: Semi-Analytic**	**Method 3: Table Look-up**	**Method 3 Graph, Equation Fit**
Apogee<2000 km	No	No	No margin req'd	5% margin	10% margin	25% margin
Apogee<2000 km	No	Yes	No margin; use SRP	5% margin ; use SRP	10% margin IFF $C_r \approx 1.7$	N/A
Apogee<2000 km	Yes	No	No margin req'd	5% margin	N/A	N/A
Apogee<2000 km	Yes	Yes	No margin req'd; use SRP	5% margin ; use SRP	N/A	N/A
Apogee>2000 km	Either	Either	No margin req'd; use 3Bdy+SRP	5% margin; use 3Bdy+SRP	N/A	N/A

(**N/A** = "*Not Applicable*"; **3Bdy**=*Third-Body Perturbations*; **SRP**=*Solar Radiation Pressure*)

Figure 4 — Applicable method with mandated conservative margins of error (in percent) and required perturbation modelling

Method 1, certainly the highest fidelity model, utilizes a numerical integrator with a detailed gravity model, third-body effects, solar radiation pressure, and a detailed satellite ballistic coefficient model. Method 2 utilizes a definition of mean orbital elements[5, 6], semi-analytic orbit theory and average satellite ballistic coefficient to permit the very rapid integration of the equations of motion, while still retaining reasonable accuracy. Method 3 is simply a table lookup, graphical analysis or evaluation of equations fit to pre-computed orbit lifetime estimation data obtained via the extensive and repetitive application of Methods 1 and/or 2.

4.2 Method 1: High-precision numerical integration

Method 1 is the direct numerical integration of all accelerations in Cartesian space, with the ability to incorporate a detailed gravity model (*e.g.*, using a larger spherical harmonics model to address resonance effects), third-body effects, solar radiation pressure, vehicle attitude rules or aero-torque-driven attitude torques, and a detailed satellite ballistic coefficient model based on the variation of the angle-of-attack with respect to the relative wind. Atmospheric rotation at the Earth's rotational rate is also easily incorporated in this approach. The only negative aspects to such simulations is (1) they run much slower than Method 2; (2) many of the detailed data inputs required to make this method realize its full accuracy potential are simply unavailable; and (3) any gains in orbit lifetime prediction accuracy are frequently overwhelmed by inherent inaccuracies of atmospheric modelling and associated inaccuracies of long term solar activity predictions/estimates. However, to analyse a few select cases where such detailed model inputs are known, this is undoubtedly the most accurate method. At a minimum, Method 1 orbit lifetime estimations shall account for J_2 and J_3 perturbations and drag using an accepted atmosphere model and an average ballistic coefficient. In the case of high apogee orbits (*e.g.*, Geosynchronous Transfer Orbits), Sun and Moon third-body perturbations shall also be modelled.

4.3 Method 2: Rapid semi-analytical orbit propagation

Method 2 analysis tools utilize semi-analytic propagation of mean orbit elements[5, 6] influenced by gravity zonals J_2 and J_3 and selected atmosphere models. The primary advantage of this approach over direct numerical integration of the equations of motion (Method 1) is that long-duration orbit lifetime cases can be quickly analysed (*e.g.*, 1 second versus 1700 seconds CPU time for a 30-year orbit lifetime case). While incorporation of an attitude-dependent ballistic coefficient is possible for this method, an average ballistic coefficient is typically used. At a minimum, Method 2 orbit lifetime estimations shall account for J_2 and J_3 perturbations and drag using an accepted atmosphere model and an average ballistic coefficient. In the case of high apogee orbits (*e.g.*, GTO), Sun and Moon third-body perturbations shall also be modelled.

4.4 Method 3: Numerical Table Look-Up, Analysis and Fit Equation Evaluations

In this final method, one uses tables, graphs and equations representing data that was generated by exhaustively using Methods 1 & 2 (see above). The graphs and equations provided in this standard can help the analyst crudely estimate orbit lifetime for their particular case of interest; the electronic access to tabular look-up provided via this standard (at www.CelesTrak.com) permits the analyst to estimate orbit lifetime for their particular case of interest via interpolation of Method 1 or Method 2 gridded data; all such Method 3 data in this paper were generated using Method 2 approaches. At a minimum, Method 3 orbit lifetime products shall be derived from Method 1 or Method 2 analysis products meeting the requirements stated above. When using this method, the analyst shall impose at least a ten-percent margin of error to account for table look-up interpolation errors. When using graphs and equations, the analyst shall impose a 25% margin of error.

4.5 Orbit lifetime sensitivity to Sun-synchronous, and high-eccentricity orbits

For sun-synchronous orbits, orbit lifetime has some sensitivity to the initial value of RAAN due to the density variations with the local sun angle. Results from numerous orbit lifetime estimations show that orbits with 6:00 am local time have longer lifetime than orbits with 12:00 noon local time by about 5.5 percent[4]. This maximum difference (500 days) translates into a 5% error which can be corrected by knowing the local time of the orbit. As a result, Method 1 or 2 analyses of the actual sun-synchronous orbit condition shall be used when estimating the lifetime of Sun-synchronous orbits.

For high-eccentricity orbits, it has been found to be difficult to iterate to lifetime threshold constraints due to the coupling in eccentricity between the third-body perturbations and the drag decay. Due to this convergence

difficulty, only Method 1 or 2 analyses shall be used when determining initial conditions which achieve a specified lifetime threshold for such orbits.

5 Atmospheric density modelling

5.1 General

The three biggest factors in orbit lifetime estimation are (1) the selection of an appropriate atmosphere model to incorporate into the orbit acceleration formulation; (2) the selection of appropriate atmosphere model inputs; and (3) determination of a space object's ballistic coefficient. We will now spend some time discussing each of these three aspects.

5.2 Atmospheric Drag Models

There are a wide variety of atmosphere models available to the orbit analyst. The background, technical basis, utility and functionality of these atmosphere models are described in detail in references 7 - 16. This standard will not presume to dictate which atmosphere model the analyst shall use. However, it is worth noting that in general, the heritage, expertise and especially the observational data that went into creating each atmosphere model play a key role in that model's ability to predict atmospheric density, which is in turn a key factor in estimating orbit lifetime. Many of the early atmosphere models were low fidelity and were created on the basis of only one, or perhaps even just a part of one, solar cycle's worth of data.

The advantage of some of these early models is that they typically run much faster than the latest high-fidelity models (Figure 5), without a significant loss of accuracy. However, the use of atmosphere models that were designed to fit a select altitude range (*e.g.*, the "exponential" atmosphere model depicted below) or models that do not accommodate solar activity variations should be avoided as they miss too much of the atmospheric density variations to be sufficiently accurate.

There are some early models (*e.g.*, Jacchia 1971 shown below) which accommodate solar activity variations and also run very fast; these models can work well for long-duration orbit lifetime studies where numerous cases are to be examined. Conversely, use of the more recent atmosphere models are encouraged because they have substantially more atmospheric drag data incorporated as the foundation of their underlying assumptions. A crude comparison of a sampling of atmosphere models for a single test case is shown in Figures 6 and 7, illustrating the range of temperatures and densities exhibited by the various models. Although this standard does not presume to direct which atmosphere model the analyst should use, the reader is encouraged to seek atmosphere model guidance from existing and upcoming ISO Standards and CIRA Working Group (e.g. CIRA-2008) recommendations. Models worthy of consideration include, but are not limited to, the NRLMSISE-00[11], JB2006[12], JB2008[13], GRAM-07[14], DTM-2000[15] and GOST[16] models.

Atmosphere Model	0<Alt<5000 km	0<Alt<1000 km
Exponential	1.00	1.00
Atm1962	1.43	1.51
Atm1976	1.54	1.54
Jacchia 1971	13.68	17.31
MSIS 2000	141.08	222.81
JB2006	683.85	584.47

Figure 5 — Comparison of normalized density evaluation runtimes

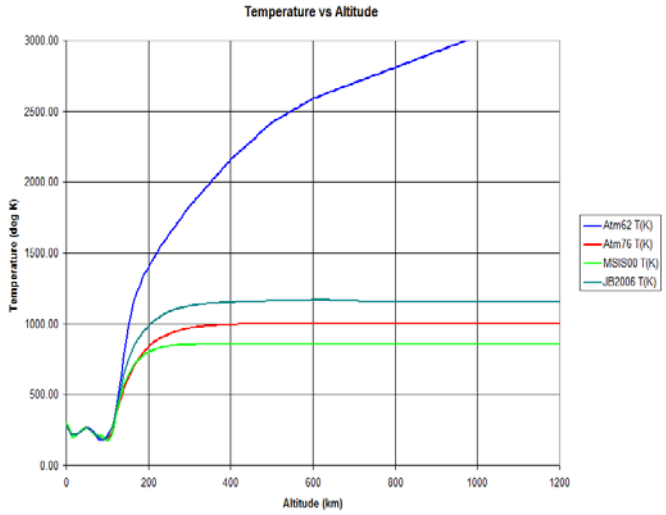

Figure 6 — Temperature comparison by atmosphere model

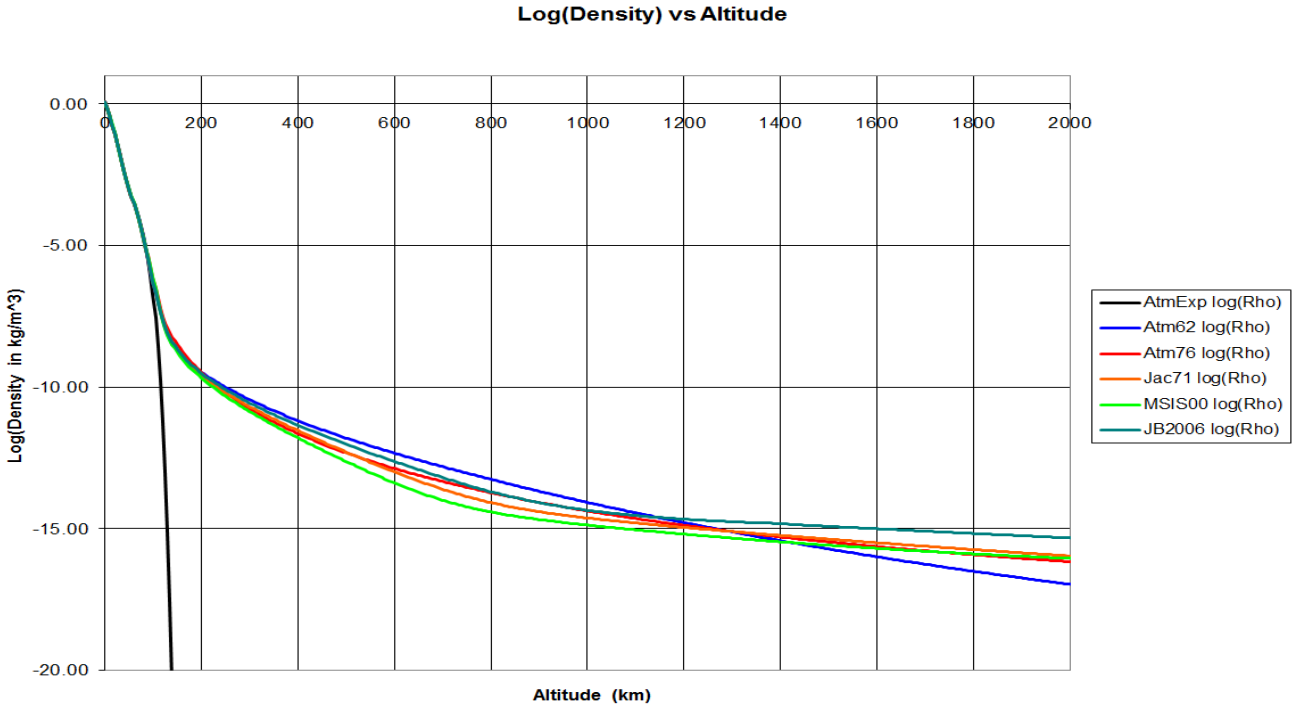

Figure 7 — Comparison of a small sampling of atmosphere models

5.3 Long-Duration solar flux and geomagnetic indices prediction

Utilization of the higher-fidelity atmosphere models mentioned in the previous subclause requires the orbit analyst to specify the solar and geomagnetic indices required by such models. Care must be taken to obtain the proper indices required by each model; subtle difference may exist in the interpretation of similarly named indices when used by different atmosphere models (*e.g.*, centrally-averaged vs. backward-averaged $F_{10.7}$ Bar).

Key issues associated with any prediction of solar and geomagnetic index modelling approach are:

b) $F_{10.7}$ Bar predictions should reflect the mean solar cycle as accurately as possible;

c) Large daily $F_{10.7}$ and A_p index variations about the mean value induce non-linear variations in atmospheric density, and the selected prediction approach should account for this fact; i.e., one should account for the highly non-linear aspects of solar storms versus quiet periods;

d) The frequency of occurrence across the day-to-day index values is highest near the lowest prediction boundary (Figure 9);

e) $F_{10.7}$ cycle timing/phase are always imprecise and should be accounted for; the resultant time bias that such a prediction error would introduce can yield large $F_{10.7}$ prediction errors of 100% or more;

f) Although still under review, the long-time duration currently being advocated by the IADC (i.e., 25 years) would require that the solar/geomagnetic modelling approach provide at least that many years (i.e., 25) of predictive capability.

g) Predicted $F_{10.7}$ values should be adjusted to correct for Earth-Sun distance variations.

h) Some atmosphere models (e.g., JB2006 & JB2008), due to the newly invented indices adopted thereby, preclude the use of historical indices for long-term orbit lifetime studies, while currently also precluding use of any predictive forecasting model(s) for those indices until such time as those become publicly available.

Accounting for these constraints, the user shall adopt one of the two approaches:

1) Approach #1: Utilize Monte Carlo sampling of historical data[17, 18] mapped to a common solar cycle period;

2) Approach #2: Utilize a predicted $F_{10.7}$ Bar solar activity profile generated by a model such as is detailed[19] in Figure 8, coupled with a stochastic or similar generation of corresponding $F_{10.7}$ and A_p values[e.g., 20].

Since Approach #2 is a well-known and common approach, the focus of the remainder of this subclause will be devoted to the Monte Carlo "Random Draw" approach[4]. Note (Figure 2) that we already have more than five solar cycles of observed solar and geomagnetic data to choose from. Processing of this data maps each coupled and correlated triad of datum ($F_{10.7}$, $F_{10.7}$ Bar, and A_p) into a single solar cycle range of 10.82546 years (3954 days), with the 'averaged' solar minimum referenced to 25 February 2007.

By mapping this historical data into a single solar cycle (Figures 10 through 12), the user can then sample coupled triads of ($F_{10.7}$, $F_{10.7}$ Bar, and A_p) data corresponding to the orbit lifetime simulation day within the mapped single solar cycle. This solar/geomagnetic data can then be updated at a user-selectable frequency (e.g. once per orbit or day), thereby simulating the drag effect resulting from solar and geomagnetic variations consistent with historical trends for these data. Since we have accumulated daily data since the February 14, 1947, on any given day within the 3954-day solar cycle we have at least five data triads to choose from. It is important that the random draw retain the integrity of each data triad, since $F_{10.7}$, $F_{10.7}$ Bar and A_p are interrelated.

In summary, the selected method used for modelling solar and geomagnetic data is to select a new coupled triad of ($F_{10.7}$, $F_{10.7}$ Bar, and A_p) data for each day (or alternately for each orbit rev) of the orbit lifetime simulation, thereby simulating the drag effect resulting from solar and geomagnetic variations consistent with historical trends for these data. The atmospheric density estimated from atmospheric models utilizing a given ($F_{10.7}$, $F_{10.7}$ Bar, and A_p) triad can then be directly utilized by either Method 1 (Numerical Integration) or Method 2 (semi-analytic) approaches. Due to the introduced step-function change in atmospheric density, it may be beneficial to restart Method 1 integration at each parameter set change; for semi-analytic (e.g., with orbital revolution time steps via Gaussian quadrature), a new parameter set can be drawn at an orbit revolution time step; thus, no numerical difficulties will be introduced. The C++ code used to implement this atmospheric variation strategy is publicly available at www.CelesTrak.com so that users of this orbit lifetime standard can adopt this standardized ($F_{10.7}$, $F_{10.7}$ Bar and A_p) implementation Approach #1 if desired.

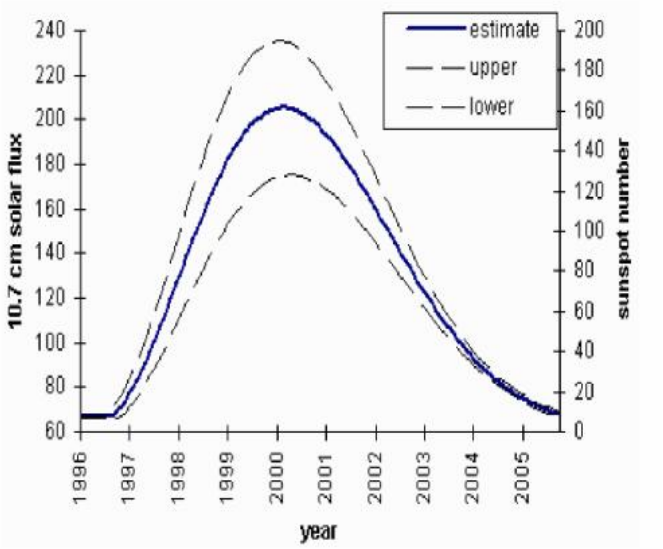

Figure 8 — Solar flux estimated upper, lower and representative trends

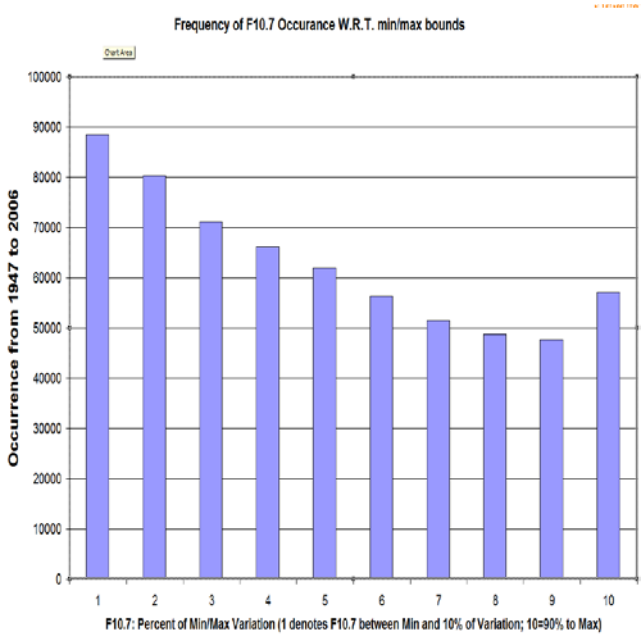

Figure 9 — Solar flux distribution in percentage of localized min/max variation

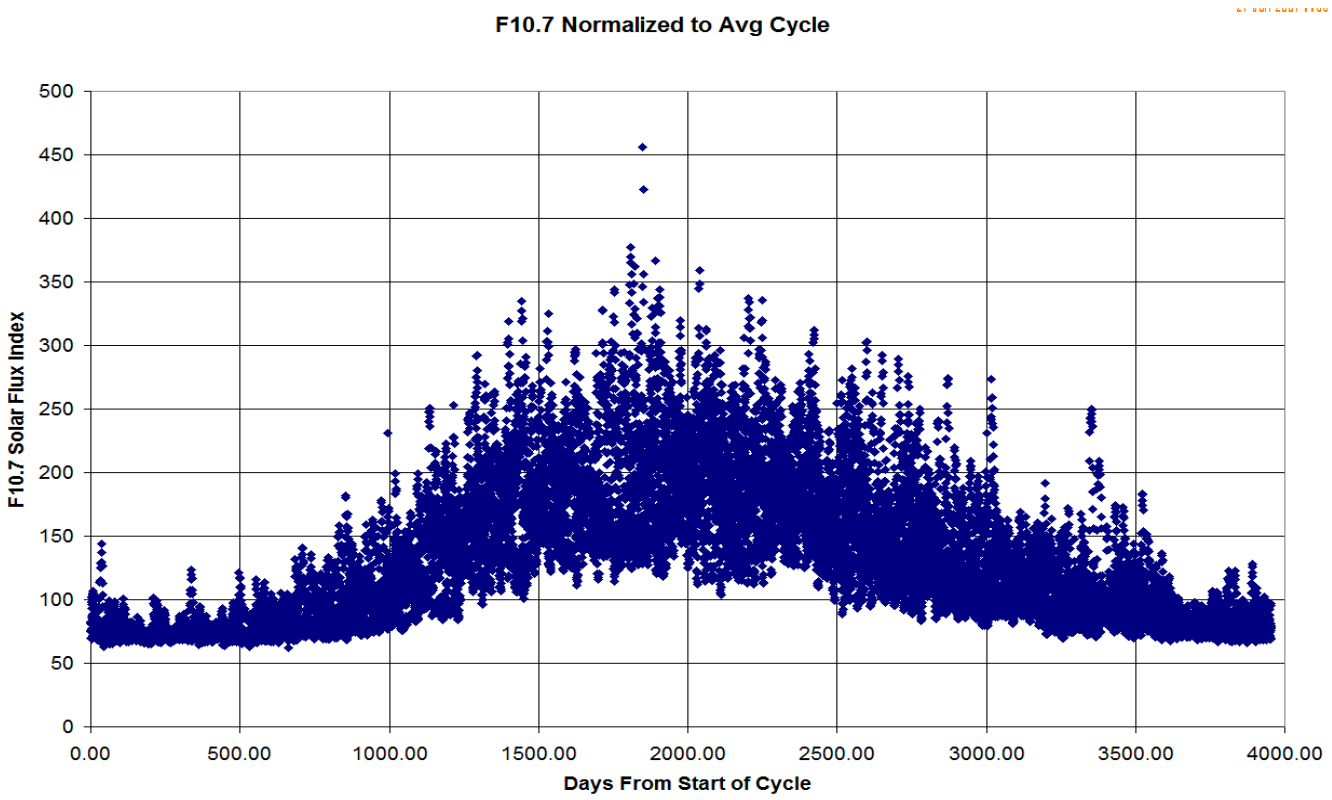

Figure 10 — F10.7 normalized to average solar cycle

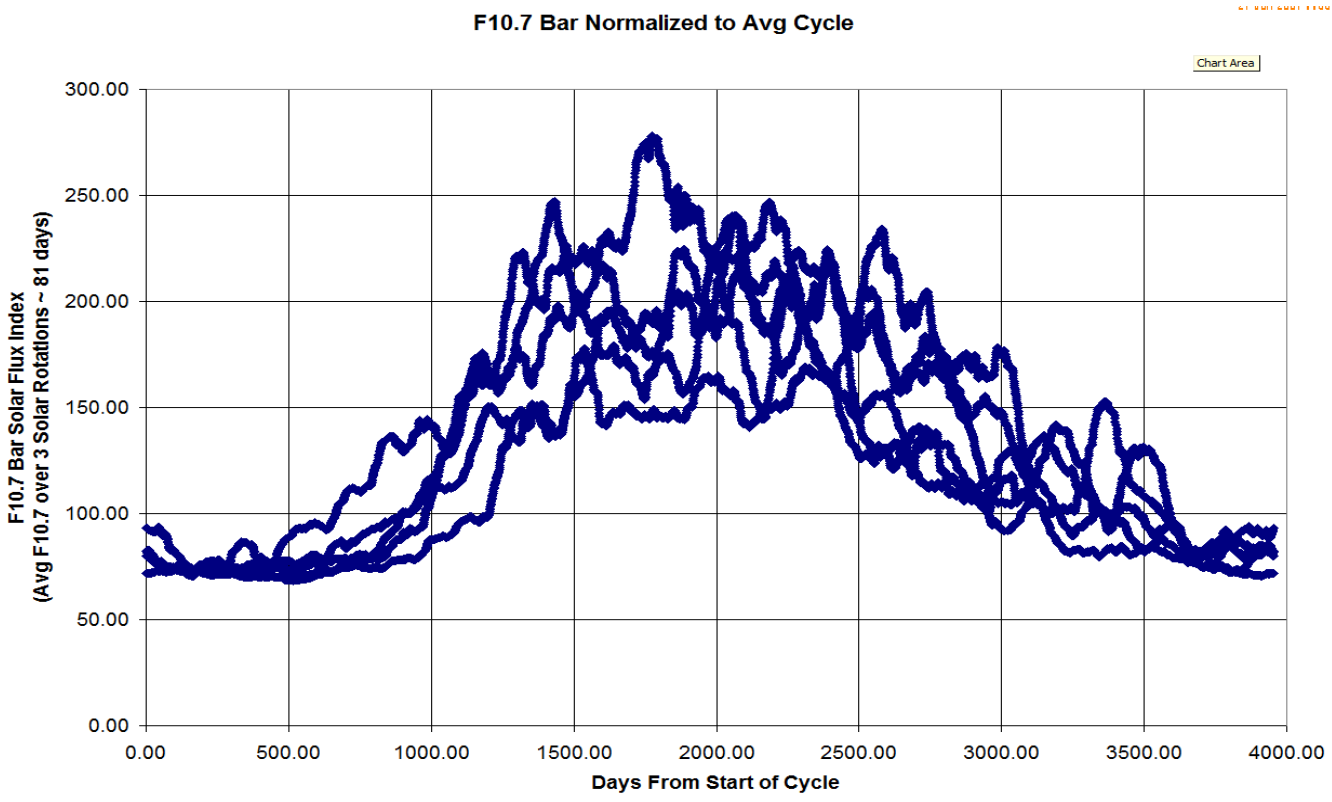

Figure 11 — F10.7 bar normalized to average cycle

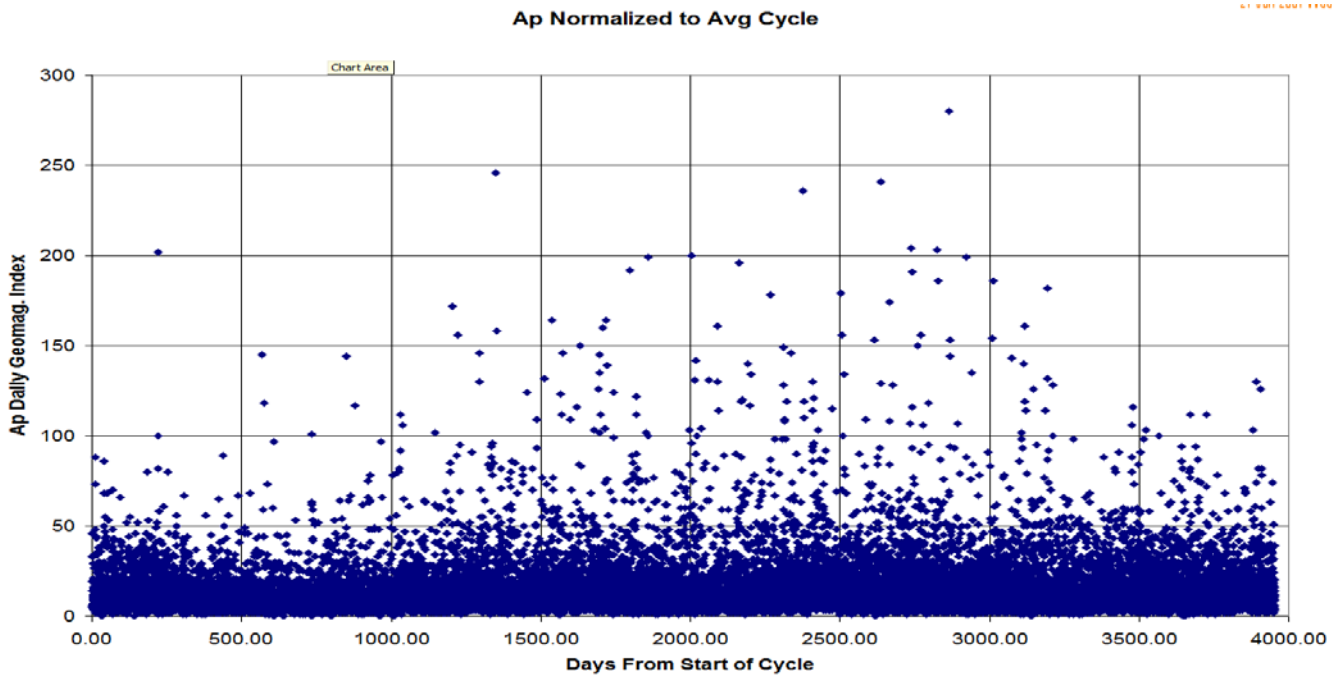

Figure 12 — A_p normalized to average cycle

It can be seen from Figure 12 that A_p is (1) unpredictable; (2) loosely correlated with the solar cycle; and (3) volatile. Figure 13 demonstrates that density varies greatly (i.e., several orders of magnitude) depending upon A_p; thus, a geomagnetic storm can induce large decreases in orbital energy (orbit decay) that the use of some average A_p value would miss. Correspondingly, the analyst should incorporate A_p variations into the geomagnetic index predictions.

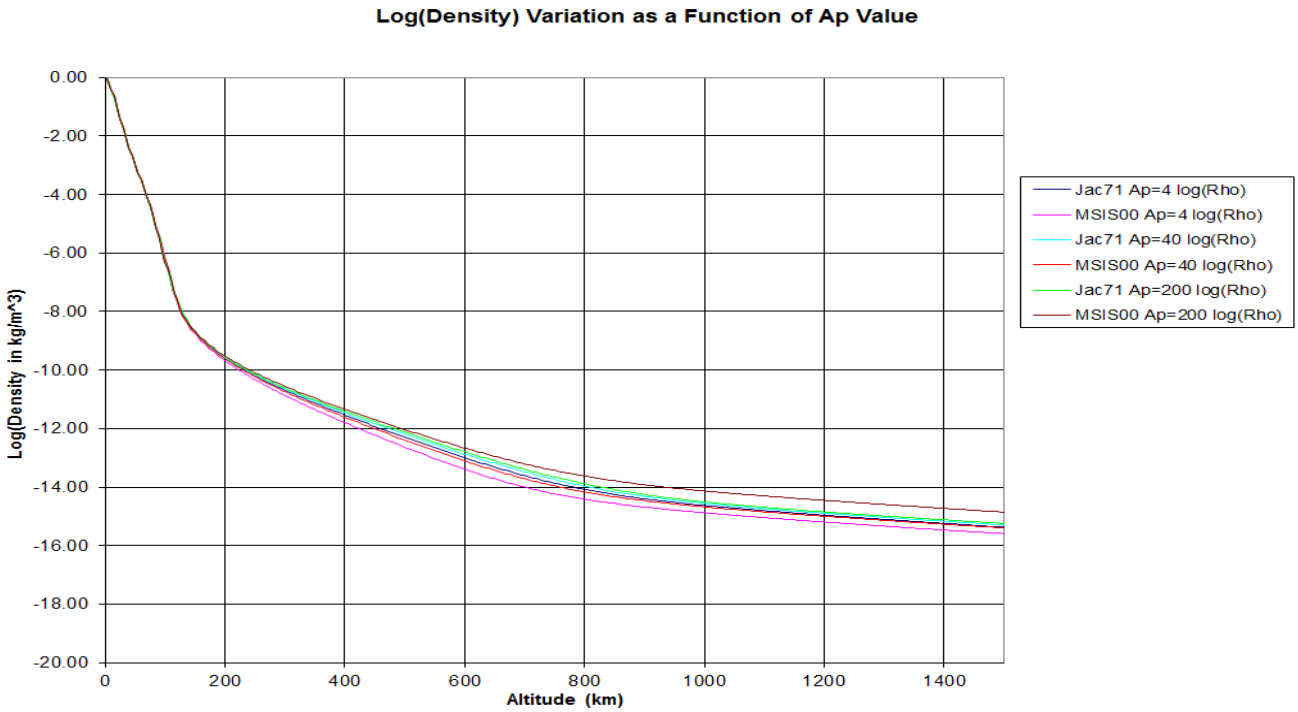

Figure 13 — Log(density) variation as a function of A_p value

5.4 Atmospheric density implications of thermospheric global cooling

Recent indications of global cooling in the thermosphere may have gradually increasing role in orbit lifetime estimation. The thermosphere is defined to occur roughly between 80 and 500 km altitude, which is a key part of the LEO regime for which the ISO standard is being developed. Both satellite measurements[15] and theoretical models[16, 17] indicate that the thermosphere is cooling off, causing density to lower. The mechanism causing this change appears to be that as CO_2 concentrations have increased (from 320 ppmv in 1965 to around 380 ppmv in 2005) at altitudes below 30km, and the upper atmosphere is correspondingly cooling down. It is estimated that because of this effect, atmospheric density will decrease by between 1.7%[21] and 2%[22, 23] per decade. This decrease yields a corresponding increase in orbit lifetime of between 4 and 7 percent[3].

6 Estimating ballistic coefficient (C_DA/m)

6.1 General

The first step in planning a LEO-crossing space object disposal is to estimate the ballistic coefficient (C_DA/m), β where:

$$\beta = (\text{Coefficient of Drag } C_D) * (\text{Object Cross-Sectional Area}) / \text{Object Mass.}$$

Accurate estimation of the space object's ballistic coefficient is another key element in the orbit lifetime analysis process. Frequently, the analyst will select an average ballistic coefficient for the duration of the prediction, but this is not always the case. We will examine cross-sectional area and drag coefficient estimations separately. Spacecraft mass shall be varied according to best-available knowledge, but may typically be assumed to be constant from End-of-Life until orbit decay.

6.2 Estimating drag coefficient

A reasonable value of the dimensionless drag coefficient, C_D, is 2.2 for a typical spacecraft. However, the drag coefficient, C_D, depends on the shape of the satellite and the way air molecules collide with it. However, for certain geometric configurations such as spheres, cylinders and cones, the value of axial drag coefficient, C_D, can be evaluated more precisely than previously noted provided something is known about the flow regime and reference area[4]. The analyst shall consider C_D variations based on satellite shape. However, for long-duration orbit lifetime estimations, C_D variation as a function of orbit altitude[4] may safely be ignored since the orbit lifetime percent error will be quite small due to averaging effects about the adopted 2.2 value.

6.3 Estimating cross-sectional area with tumbling and stabilization modes

The ballistic coefficient has a sensitive impact on the orbit lifetime. Average cross-sectional area is one of three key components (the others being mass and drag coefficient) which comprise the ballistic coefficient. In this subclause, we examine how average cross-sectional area should be estimated.

If the attitude of the spacecraft can't be anticipated (as is typically the case), the user shall compute a mean cross-sectional area assuming that the attitude of the spacecraft may vary uniformly (relatively to the velocity direction) i.e. that all the possible attitudes may be achieved with the same probability and during the same time. The mean cross-sectional area is obtained by integrating the cross-sectional area across a uniform distribution of attitude of the spacecraft (as if an observer would observe a spacecraft from any direction and compute the resulting mean observed cross-section).

In the absence of a more detailed model, a composite flat-plate model may be utilized. For example, for a plane sheet of which S is the area, it can be demonstrated that the "mean surface area" is S/2 when averaged over all possible viewing angles; by extension, for a parallelepiped-shaped spacecraft, S1, S2, S3 being the three surfaces (their opposite sides are to be neglected because when a side is visible, the opposite one is masked), it can be demonstrated that this "mean surface area" is (S1+S2+S3)/2; if a solar array of surface S4 is added, the mean surface area is then (S1+S2+S3+S4)/2 (neglecting any possible masking between the solar array and the spacecraft). This flat plate model has been shown to be accurate to within 20% for tracked

objects. Since masking effects represent a systematic bias that has the effect of reducing drag (thereby increasing orbit lifetime), an appropriately conservative cross-sectional area masking reduction factor shall be introduced to maintain accuracy.

To eliminate the need for such conservatism, this plate model approach can be extensively refined by integrating the cross-sectional area of the spacecraft across all anticipated tumbling attitudes (e.g. using a Computer-Aided Design or CAD program), and then dividing the result by the difference between the limits of integration. The analyst is then left with a properly weighted average cross-sectional area.

For satellites with a large length to diameter ratio, the analyst shall consider whether gravity gradient stabilization will occur and adjust the cross-sectional area based upon the anticipated stabilized geometry. Similarly, for satellites which have a large aero-torque moment (*i.e.*, the center-of-gravity and center-of-pressure are suitably far apart and the aerodynamic force is suitably large), the analyst shall consider whether the satellite would experience drag-induced passive attitude stabilization and adjust the cross-sectional area accordingly.

6.4 Estimating mass

The mass of the spacecraft shall be assumed to be its total mass at mission completion, where total mass is comprised of the spacecraft's dry mass plus the anticipated fuel margin of safety upon completion of the spacecraft's deorbit or safing maneuvers.

Annex A
(informative)

Space population distribution

The launch vehicle and its family of deployed objects pass through various orbit regimes during the ascent phase from launch up to the mission orbit. As can be seen in Figures A.1 and A.2, the collision risk is especially high in specific orbital regimes (the LEO and GEO belts and at the altitudes of deployed constellations).

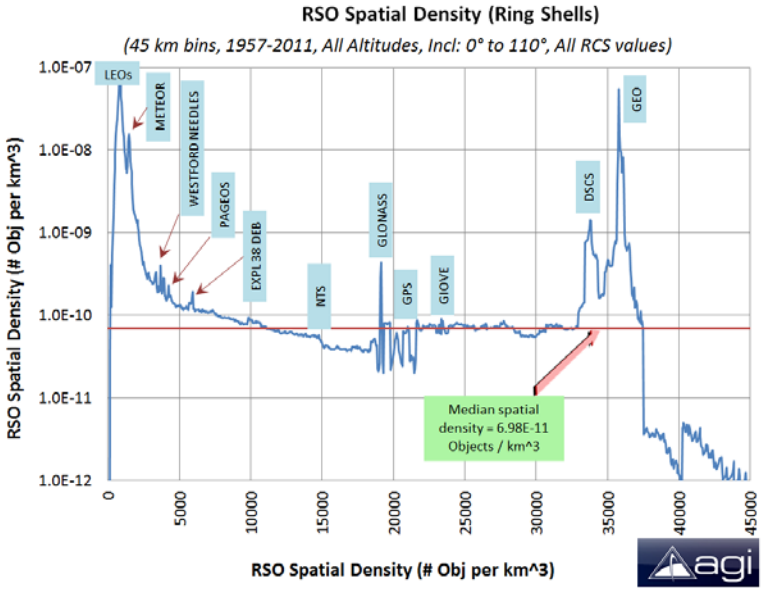

Figure A.1 — Sample near-earth space spatial density, 2011

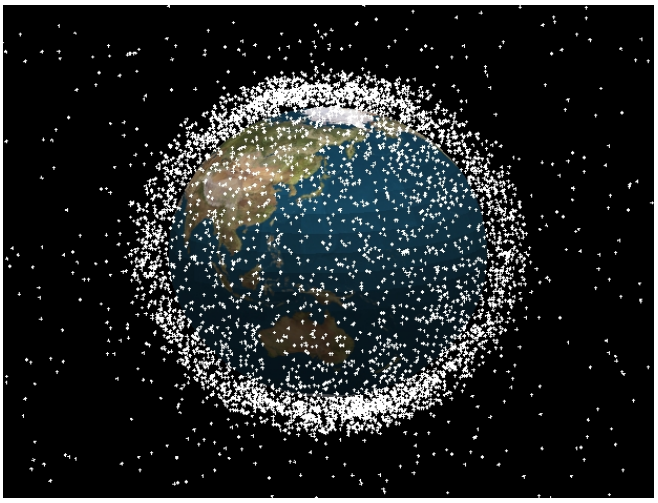

Figure A.2 — Distribution in low-Earth orbit

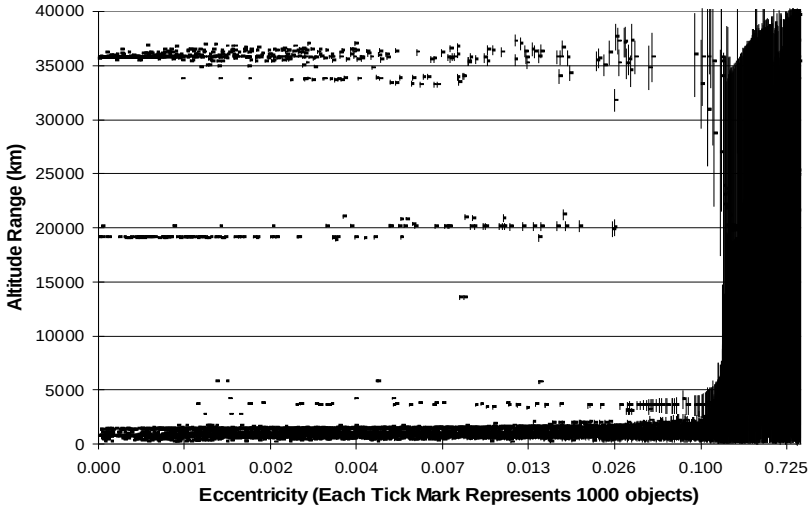

Figure A.3 — Space population by altitude and eccentricity

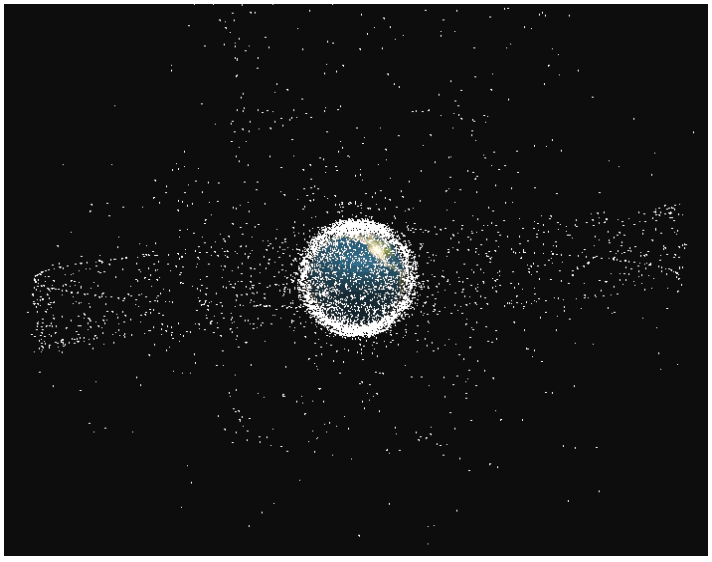

Figure A.4 — Distribution in near-Earth space

Annex B
(informative)

25-Year lifetime predictions using random draw approach

If the user of this standard wishes to estimate whether a space object has a 25-year orbit lifetime or not, a set of Method 3 analysis products have been generated and are available in this Annex. This Method 3 data was generating utilizing solar/geomagnetic modelling Approach #1, coupled with a Method 2 orbit lifetime analysis tool (1Earth Research semi-analytic orbit propagator 'QPROP'). QPROP was used to examine the 8 million cases contained in Table B.1, spanning a variety of times-into-the-solar-cycle, inclinations, perigee altitudes (H_p), apogee altitudes (H_a), and ballistic coefficients. QPROP uses semi-analytic propagation of mean orbit elements coupled with gravity zonals J_2 and J_3 and selected atmosphere models (including NRLMSISE-00, Jacchia-Bowman, Jacchia 1971, etc). QPROP has been used to analyse orbit lifetime and satellite re-entry by several Government and industrial organizations. Its accuracy has been validated by high-precision numerical integration results (Method 1 type).

Figure B.1 — QPROP grid of test cases

Parameter	***Lower Limit***	***Upper Limit***	***Step Size***
Time into Solar Cycle (days)	0	2964.75	3953/4
Inclination (deg)	0	90	30
C_DA/m (cm^2/kg)	25	500	25.
Perigee Altitude (km)	100	2000	50
Apogee Altitude (km)	250.	10000	50
Number of Trials	0	3	1

The primary independent variables of the orbit lifetime estimation process are contained in Table B.1. By stepping through all of these variables in the ranges and step sizes indicated in the table, and then detecting those cases which resulted in a 25-year orbit lifetime, the dependencies between ballistic coefficient and orbit initial condition can be found. While both the NRLMSISE-00 and Jacchia-Bowman atmosphere models are implemented in QPROP, the NRLMSISE-00 model was used for these analyses due to its faster runtime with similar long-term propagation accuracy. Random draws of the triad of solar and geomagnetic index parameters (discussed in subclause 5.3) were implemented. In order to capture variations exhibited by the random draw process, a number of trials were used (four, in this case).

For a satellite having a ballistic coefficient of 200 cm^2/kg and starting in a circular, equatorial orbit at the altitude shown, Figure B.1 depicts the resultant ranges of anticipated orbit lifetime. The 'minimum' and 'maximum' incorporates the entire range of orbit decay start times with respect to the solar cycle minimum. The right-hand side of the plot shows how variable the results can get in the neighbourhood of 25 years estimated lifetime.

The dependence of orbit lifetime upon orbit inclination is shown for the same 200 cm^2/kg sample case in Figure B.2. In Figure B.2, it is seen that polar orbits experience reduced atmospheric drag, likely due to both the reduced time spent flying near the solar sub-point in combination with the reduced atmospheric density at the Earth's poles due to the oblate shape of the Earth and atmosphere**.**

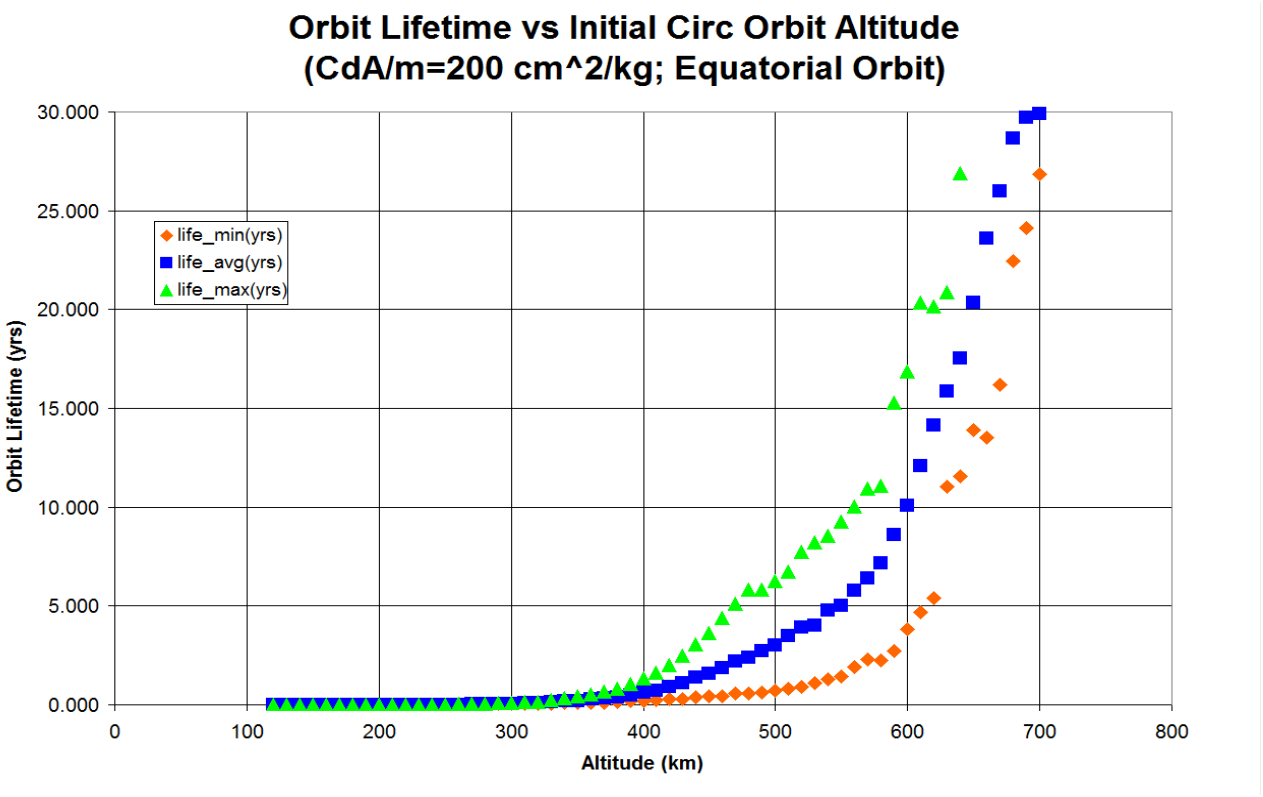

Figure B.2 — Sample orbit lifetime (CDA/m = 200 cm2/kg, equatorial orbit) as a function of initial orbit altitude

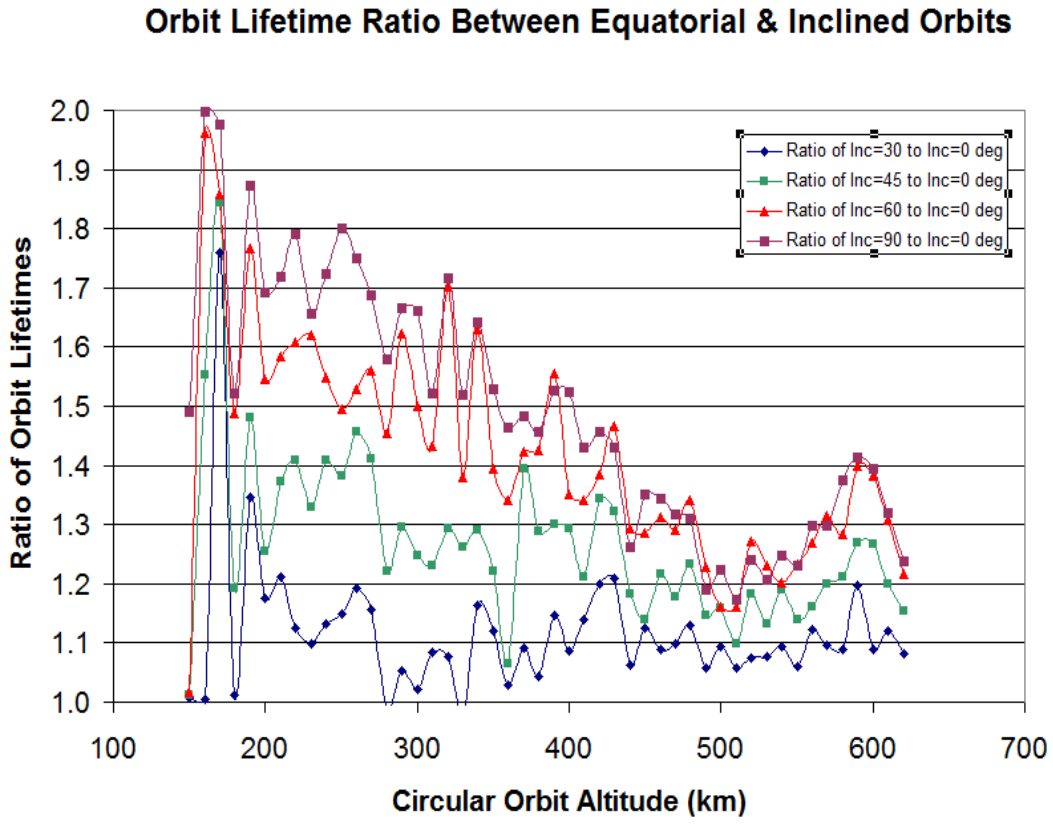

Figure B.3 — Orbit lifetime dependence upon orbit inclination

Future studies may use more trials and incorporate finer step sizes, but the large computer runtime requirements of these many cases led to the initial selection of 4 trials per initial set of orbit conditions. Through extensive simulation, it was found for **non-Sun-Synchronous** orbits that orbit lifetime results are not sensitive to the three angular orbit elements (RAAN, argument of perigee and mean anomaly) and therefore the three initial values are arbitrarily chosen and assumed for all cases. Note that the sensitivity to RAAN and argument of perigee may be significant for sun-synchronous, and more generally for high-eccentricity orbits; this was discussed in subclause 4.5. NOTE: It is recommended that Sun-Synchronous orbit cases be studied using a 'Method 1' or '2' approach; until such time as their orbit lifetimes can be appropriately categorized in graphical and/or functional form. Further, it was found that orbits having inclinations greater than 90 degrees could be well-represented by the pole-symmetric orbits having complementary orbit inclinations (justifying analysis of only 0 to 90 degrees as shown in Table B.1).

The colored regions shown in Figures B.3 and B.4 denote the categorization of the orbit initial conditions at the start of the orbit decay with respect to the IADC 25-year recommended post-mission lifetime. The 'green' region denotes orbit initial conditions which will result in an orbit lifetime shorter than 25 years (in all observed cases). The 'yellow' region denotes initial orbit conditions that could result in an orbit lifetime that is greater than the recommended 25-year limit, in certain circumstances.

One can observe from Figures B.3 and B.4 that there are a wide variety of initial orbit, timing, solar and geomagnetic conditions which can combine to produce an orbit lifetime of 25 years. These figures, while helpful, still leave the user with uncertain knowledge of what the post-mission orbit lifetime will be specific to their initial conditions. Fortunately, the results of the 7.68 million analyses have been retained[4]; interpolation of these results is possible to predict orbit lifetime for a specific set of initial conditions. And, to the extent that 4 sets of random draw cases is not necessarily an exhaustive analysis, additional cases can be run to further refine the orbit lifetime estimation grid and improve interpolation results.

Orbit lifetime data generated by the many analysis runs can be fit with a set of analytical expressions which predict average orbit lifetime (in years) as a function of H_p, inclination, ballistic coefficient and orbit eccentricity[4]. Note, however, that the resulting set of equations exhibits a peak deviation of up to 100% from the underlying estimated lifetime data in extreme cases, coupled with an average standard deviation of less than 20% error above 200 km. The effort invested in obtaining this unsuitable result indicates that a better approach would be to not fit the data, but rather to: (1) use the Method 2 analysis tool to entirely map out the orbital lifetime topography[24]; (2) store the lifetime topography data electronically; and (3) provide space operators with a simple and fast electronic access to a topography interpolation function.

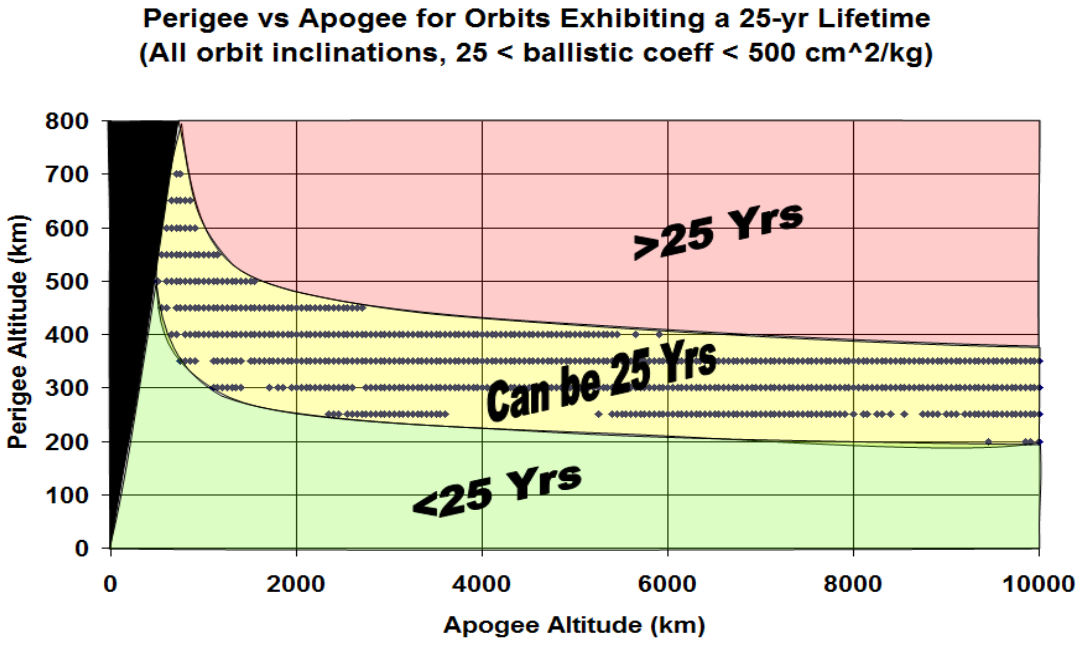

Figure B.4 — Perigee versus apogee boundaries for 25-year orbit lifetime conditions (25 < CDA/m < 500 cm2/kg)

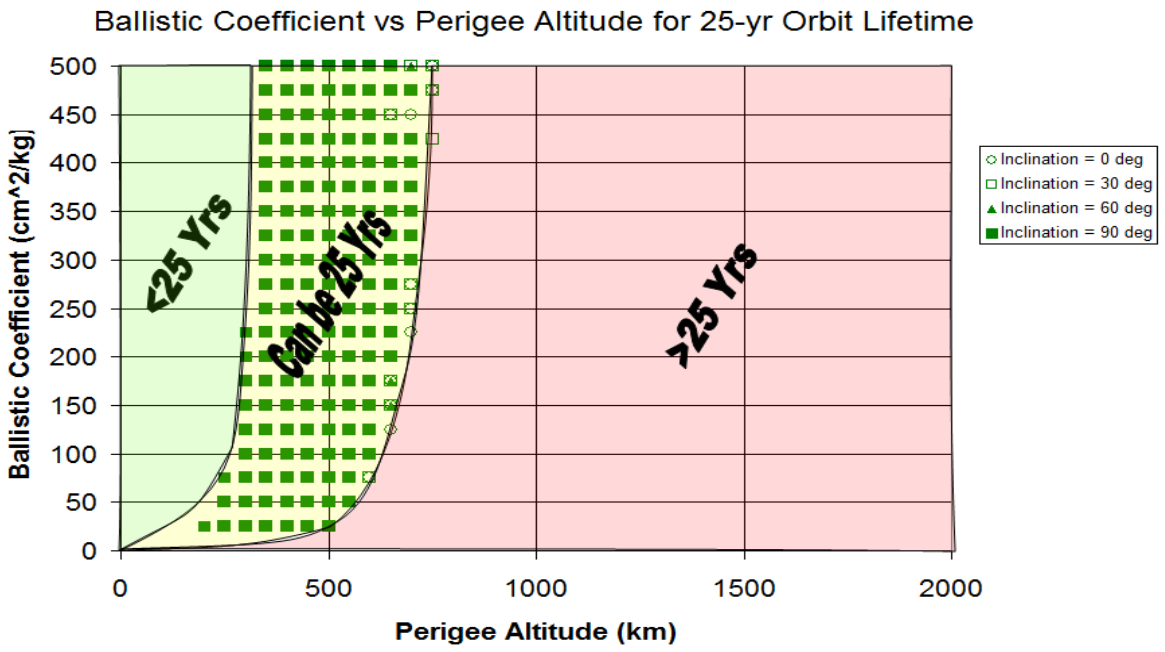

Figure B.5 — Ballistic coefficient versus initial perigee altitude for all cases exhibiting 25-year orbit lifetime (apogee assumed < 10,000 km)

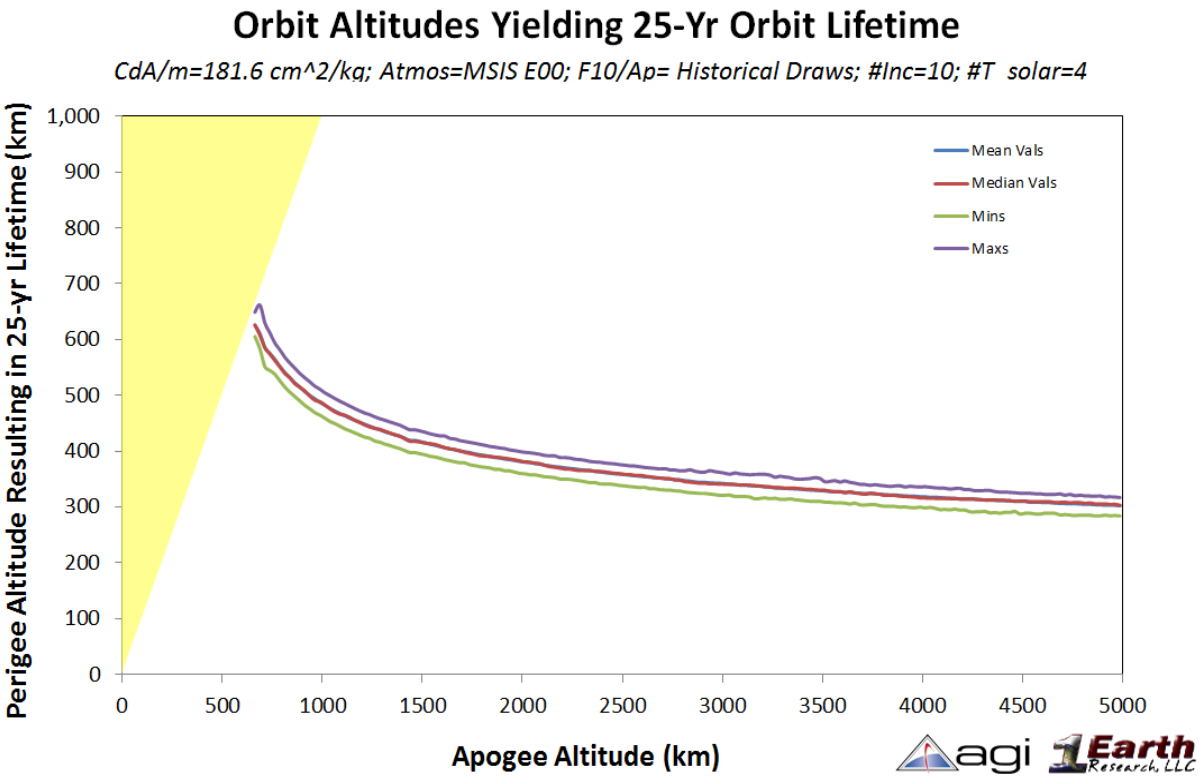

Figure B.6 —Median 25-Year Orbit Lifetime Statistics For Ballistic Coefficient of 181.6 cm^2/kg

Annex C
(informative)

Solar radiation pressure and 3rd-body perturbations

C.1 Solar radiation pressure modeling

For orbits with high eccentricity or high area-to-mass ratios, it is recommended that the analyst include perturbations due to Solar Radiation Pressure (SRP). A number of modelling resources can be found[25, 26]. Implementations of such models can be checked against well-documented on-orbit observations[18]. Figure C.1 shows variations in orbital elements for the Dash-2 satellite mission (1964) using both Method 1 numerical integration (SPIN) and Method 2 semi-analytic (OPUS) approaches. As eccentricity and semi-major axis fluctuate due to SRP, perigee can become low enough in some cases that the satellite re-enters.

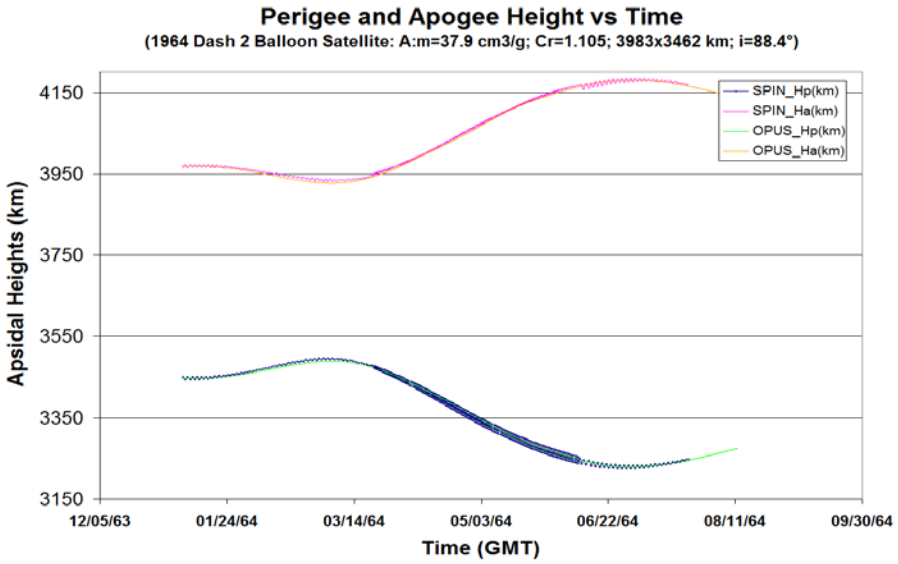

Figure C.1 — SRP-induced variation in mean orbit elements for 1964 Dash-2 satellite

C.2 3rd-body modeling

Gravity contributions to the forces on an Earth-orbiting spacecraft are typically modeled using a gravity field for the Earth and point-mass third-body gravity forces arising from the Moon and Sun. Let B_i be a celestial body and $\mathbf{R}_{Bi}$ locate its (center-of-mass) position with respect to the inertial axes. The Newtonian equations of motion[27] for a spacecraft are:

$$m\ddot{\mathbf{R}} = \mathbf{F}_S + \sum_{i=0} GmM_{Bi} \frac{\mathbf{R}_{Bi} - \mathbf{R}}{\left\|\mathbf{R}_{Bi} - \mathbf{R}\right\|^3}$$

where m is the spacecraft mass, G the universal gravitation constant, M_{Bi} is the mass of B_i, and F_S is the sum of all forces on the spacecraft other than the point-mass gravitational force caused by all the celestial bodies (e.g., additional gravitational forces over the point-mass effect, drag, solar radiation pressure, general relativistic corrections, etc.).

Note that the motions of the celestial bodies are taken to be known as a function of time, so that a suitable planetary ephemeris predictor is required to evaluate the third-body accelerations.

Bibliography

[1] Inter-Agency Space Debris Coordination Committee, “IADC Space Debris Mitigation Guidelines, Revision 1”, IADC-02-01, September 2007.

[2] Space Debris Mitigation Guidelines of the Scientific and Technical Subcommittee of the Committee on the Peaceful Uses of Outer Space, Annex IV of A/AC.105/890, p.42ff, 6 March 2007, endorsed by the United Nations General Assembly under Resolution A/RES/62/217 on 10 January 2008.

[3] ISO 24113, Space systems -- Space debris mitigation requirements

[4] Oltrogge, D.L. and Chao, C.C., “Standardized Approaches for Estimating Orbit Lifetime after End-of-Life”, AAS/AIAA Astrodynamics Specialists Conference, Mackinac Island, MI, August 2007.

[5] Kozai, Y., “The Motion of a Close Earth Satellite”, Astronomical Journal 64, 367—377, November 1959.

[6] Orbital Motion – 2nd Edition, Roy, A.E., Publ. by Adam Hilger, Ltd, Bristol, ISBN 0-85274-462-5, 1982.

[7] ANSI/AIAA Guide to Reference and Standard Atmosphere Models, ANSI/AIAA document #G-003B-2004

[8] Marcos, Frank A., Bowman, Bruce R., Sheehan, Robert E., “Accuracy of Earth’s Thermospheric Neutral Density Models,” AIAA 2006-6167, AIAA/AAS Astrodynamics Specialist Conference, Keystone, Colorado, 2006.

[9] NASA Atmosphere model comparisons, URL: http://modelweb.gsfc.nasa.gov/atmos/atmos_index.html, [cited 28 Sept 2007].

[10] WG4 ISO Standard on atmosphere models (TBS).

[11] J.M. Picone, A.E. Hedin, D.P. Drob, and A.C. Aikin, "NRL-MSISE-00 Empirical Model of the Atmosphere: Statistical Comparisons and Scientific Issues," J. Geophys. Res., doi:10.1029/2002JA009430, in press (2003).

[12] Bowman, B. R., Tobiska, W. K., Marcos, F. A., Vallares, C. The JB2006 empirical thermospheric density model, Journal of Atmospheric and Solar-Terrestrial Physics 70 (5), 774-793, 2008.

[13] Bowman, B. R., Tobiska, W. K., Marcos, F. A., Huang, C.Y., Lin, C.S. & Burke, W.J., New Empirical Thermospheric Density Model JB2008 Using New Solar and Geomagnetic Indices, AIAA 2008-6438, AIAA/AAS Astrodynamics Specialist Conference, Honolulu, Hawaii, August 2008.

[14] Justus, C.G. and Leslie, F.W., The NASA MSFC Earth Global Reference Atmospheric Model—2007 Version, NASA/TM—2008–215581, November 2008.

[15] Bruinsma, S., Thuillier, G., and Barlier, F., The DTM-2000 empirical thermosphere model with new data assimilation and constraints at lower boundary: accuracy and properties, Journal of atmospheric and solar-terrestrial physics ISSN 1364-6826, 2003, vol. 65, no. 9, pp. 1053-1070.

[16] Cefola, P., Volkov, I. I., and Suevalov, V. V., Description of the Russian Upper Atmosphere Density Model GOST-2004, 37th COSPAR Scientific Assembly, Montreal, Canada, July, 2008.

[17] “2800 MHz SOLAR FLUX,” dated 20 October 2006, URL: ftp://ftp.ngdc.noaa.gov/STP/SOLAR_DATA/ SOLAR_RADIO/FLUX/read.me [cited 14 March 2007].

[18] "Gottingen K_p /A_p values," dated 20 October 2006, URL: ftp://ftp.ngdc.noaa.gov/STP/GEOMAGNETIC_DATA/ INDICES/KP_AP/read-me.txt [cited 14 March 2007].

[19] Niehuss, K.O., Euler Jr., H.C., and Vaughan, W.W., "Statistical Technique for Intermediate and Long-Range Estimation of 13-Month Smoothed Solar Flux and Geomagnetic Index," NASA Technical Memorandum TM-4759, dated September 1996.

[20] Woodburn, J. and Lynch, Shannon, "A Numerical Study of Orbit Lifetime," AAS/AIAA Astrodynamics Specialists Conference, Lake Tahoe, AAS 05-297, 2005.

[21] Marcos, F.A., Wise, J.O., Kendra, M.J., Gossbard, N.J., and Bowman, B.R.., "Detection of a long-term decrease in thermospheric neutral density," *Geophysical Research Letters*, Vol. 32, L04103, doi:10.1029/2004GL021269, 2005.

[22] Qian, Liying, Roble, Raymond G., Solomon, Stanley C., and Kane, Timothy J., "Calculated and Observed Climate Change in the Thermosphere, and a Prediction for Solar Cycle 24," *Geophysical Research Letters*, Vol. 33, L23705, doi:10.1029/2006GL027185, 2006.

[23] Solomon, Stanley C., Qian, Liying, and Roble, Raymond G., "Thermospheric Global Change during Solar Cycle 24," AGU Fall Meeting, San Francisco, CA, 12 December 2006.

[24] Finkleman, D. and Oltrogge, D, "Twenty-five Years, more or less: Interpretation of the LEO Debris Mitigation 25-Year Post-Mission Lifetime Guideline," AAS/AIAA Astrodynamics Specialist Conference, Toronto, Canada, 2010.

[25] Aksnes, K., "Short-Period and Long-Period Perturbations of a Spherical Satellite Due to Direct Solar Radiation," Center for Astrophysics, Harvard College Observatory and Smithsonian Astrophysical Observatory, Cambridge, Mass. 02138, U.S.A, 1975.

[26] Orbital Mechanics – 2nd Edition, Chobotov, V.A., editor, AIAA Education Series, ISBN 1-56347-179-5, 1996.

[27] Correct Modeling of the Indirect Term for Third-Body Perturbations, Berry, M., and Coppola, V.T, AAS 07-417, 2007.